PAPER

CrossMark
click for updates

Fabrication of superhydrophobic polycaprolactone/beeswax electrospun membranes for high-efficiency oil/water separation†

Reshmi C. R., Suja P. Sundaran, Juraij A. and Sujith Athiyanathil*

In this work, a novel superhydrophobic, superoleophilic electrospun nanofibrous membrane of beeswax and polycaprolactone has been successfully fabricated. The prepared membrane can separate oil from contaminated water with high separation efficiency and good recyclability. The hybrid membrane containing 25 wt% beeswax (PCL–25BW) possesses superhydrophobicity with a water contact angle of about $153° \pm 2$. PCL–25BW membrane exhibited high oil sorption capacity of $16.95–31.05$ g g^{-1} in different oils. Moreover, it also showed high potential for gravity driven oil–water separation with 98.1% separation efficiency. PCL–25BW membrane exhibits reusability after 15 cycles of oil sorption and gravity driven oil–water separation. The developed membrane showed an increase in tensile strength after oil sorption and environmental durability in harsh conditions such as UV exposure and pH. This work introduced a new idea to fabricate oil–water separation membranes from beeswax, which have potential in industrial oily waste water and oil spill cleanup.

1. Introduction

Superhydrophobic surfaces observed in nature such as lotus leaves, duck feathers and insect cuticles often provide inspiration for researchers. Meanwhile the fabrication of an artificial superhydrophobic surface has also received an enormous deal of attention in fundamental research due to its low surface energy, high surface roughness and gained potential applications in the fields of self-cleaning, antifouling, corrosion resistance, and oil–water separation.[1–6] An attempt has been made to fabricate micro–nanocomposite superhydrophobic films in which natural material is one of the components.[7,8] In this study beeswax is introduced as a novel natural candidate for inducing superhydrophobicity in electrospun polymer membranes. Beeswax (BW) is one among the natural waxes used in different fields like drug delivery systems, cosmetics, food packaging, photoprotectant and protective material due to its unique properties.[9–14] It comprises of multiple components like long chain hydrocarbons, alcohols, free acids, and esters. Over 95% of all carbons in beeswax are internal chain methylene [int-(CH_2)] carbons and this structure is responsible for the superhydrophobic nature of the beeswax. Beeswax is the primary waist product from honey industry with enormous applications.

So it is economical and is an easily accessible natural product comes under the category of solid lipid with low surface energy, which is composed of physiological and compatible lipids with a high melting point as the solid core.[15,16]

Recently superhydrophobic surface structures with diverse functionalities have aroused a broad attention in the separation of oil from water either by absorption or filtration.[17] Massive production of oil polluted water in oil refineries and other industries are a major problem, which not only causes energy loss, but also adversely affects the ecological environment and aquatic organism. Physical absorption of oil with super-hydrophobic–superoleophilic sorbent has been considered as an efficient technique due to its advantageous such as low operation cost and negligible secondary pollutant generation.[18,19] Materials such as sponges,[20,21] metallic wire meshes,[23,24] aerogels[25] and carbon nanotubes[26] and polymer membranes[27] are also used for oil–water separation but have some undesirable sides like large pore size and restricted recyclability.[20–27] The most important property that needs to be manipulated for efficient oil–water separation is super-hydrophobicity, which can be easily adjusted by controlling the surface energy and the surface roughness of the material.

Superhydrophobic surface fabricated by electrospinning technique have several advantages such as nanoscale rough surface morphology, high porosity, submicron pore sizes, large surface area to volume ratio and high permeability. By employing electrospinning several superhydrophobic nano-fibrous membranes including polyvinylidene fluoride,

Materials Research Laboratory, Department of Chemistry, National Institute of Technology Calicut, Calicut-673601, Kerala, India. E-mail: athiyanathil.sujith@gmail.com; Fax: +91 495 2287250; Tel: +91 9846475675

† Electronic supplementary information (ESI) available: Video S1–S3. See DOI: 10.1039/c6ra26123j

fluorinated benzoxazine, poly(methyl methacrylate) copolymer, polystyrene/polyacrylonitrile, polyurethane have been prepared.[28–34] In order to reduce surface energy and induce superhydrophobicity in electrospun membranes, complex strategies like surface functionalization, blending with inorganic nanoparticles and coaxial electrospinning has been adapted.[35–38] But most of these strategies needed complicated synthetic procedures with harmful chemicals, high cost, as well as being unsuitable for practical applications because of their low stability and poor selectivity in harsh environmental conditions. Meanwhile, in this study a simple blending strategy of natural lipid beeswax with polycaprolactone (PCL) have been adapted to fabricate a superhydrophobic membrane for effective oil water separation. Among many biodegradable polymers polycaprolactone (PCL) can be considered as a better candidate for making superhydrophobic oil–water separation membranes due to its high mechanical and thermal stability. In addition to that PCL possess a wide range of interesting features including UV and chemical resistance, low water absorption which makes it as a promising component to fabricate superhydrophobic membranes.[39]

In this study, we present the fabrication of superhydrophobic electrospun nanofibrous membranes with high water/oil separation efficiency by combining the properties of both PCL and beeswax. The effect of beeswax contents on PCL was evaluated by morphology, surface wettability analysis. The combination of PCL/beeswax could create a hierarchical roughness on the membranes surface due to its lower fiber diameter and high porosity. The developed membrane has high oil absorption and holding capacity and oil–water mixture can be separated with high efficiency. PCL/BW electrospun membranes withstand superhydrophobic characteristics in harsh conditions such as UV exposure, different pH ranges and saline water. So PCL/BW electrospun membrane has a potential for replacing the conventional oil–water separation membranes in the near future.

2. Experimental

2.1. Materials

Polycaprolactone (PCL) was obtained from Sigma-Aldrich, USA. The solvents such as dichloromethane (DCM) and dimethylformamide (DMF) were purchased from Avera Chemicals, India and Merck, India respectively. All the chemicals used are received without further purification. Beeswax (BW) was collected from local areas (Kerala, India) and purified by filtration after heating at 70 °C in a water bath (details in S1†).

2.2. Fabrication of PCL–BW nanofibers

The electrospinning solution of PCL/BW was prepared by dissolving BW in DCM by vigorous stirring for 4 h. PCL was added to the solution followed by dropwise addition of DMF, in order to prevent the precipitation of BW from the solution. The PCL/BW solution concentration was fixed to 10% (w/v). Six different solutions were prepared with varying beeswax content from 0 to 25 wt%. The clear PCL/BW solution was then placed in a 10 mL

syringe fitted with a needle having an internal diameter of 0.2 mm and pumps the solution at a controlled flow rate of 1 mL h^{-1}. The needle was connected to a voltage of 18 kV and the spun fibers are collected on the rotating collector placed at a distance of 12 cm from the needle tip. The electrospun nanofibers were collected carefully and kept in a vacuum oven at 40 °C to remove residual solvent. The prepared sample formulations have been explained in Table 1.

2.3. Characterization

The morphological structures of electrospun nanofibrous membranes were examined by field emission scanning electron microscopy (FE-SEM, Hitachi 6600) at an accelerating voltage of 10 kV. The SEM images were analyzed using the image J software and the average fiber diameter was calculated from at least 50 fibers. Surface roughness analyses have been performed by Atomic Force Microscope (AFM 110 a Park Model XE 100) in non-contact mode. The dried membranes were scanned 5 μm × 5 μm area. The infrared spectra of the electrospun membranes were obtained by using a Fourier transform infrared spectrometer (Nicolet 5700) in ATR-FTIR mode. The scans were recorded between 4000 and 400 cm^{-1}. The thermal properties of the samples were investigated by a thermogravimetric analyzer (TGA, TA Instruments, Q50) by heating samples from room temperature to 700 °C at the rate of 10 °C min^{-1} under a nitrogen flow of 60 mL min^{-1}. The mechanical properties of electrospun scaffolds of dimension 0.5 × 5 cm were investigated by a mechanical testing machine (Schimadzu Autograph, AG-Xplus series) with an applied load of 10 N. The hydrophobicity of the membrane was evaluated using static water contact angle measurement instrument (Digidrop). The water contact angle (WCA) with water volume of 3 μL and sliding angle (SA) with water volume of 10 μL were measured for the analysis of hydrophobic character of the membrane. Snaps were taken and the contact angle was determined using sessile drop method by a software program. The porosity of the electrospun membrane were calculated (details in S3†).

2.4. Oil sorption experiments

The absorption capacity of PCL/BW nanofibrous membranes were determined by placing a small piece of electrospun membrane (1 × 1 cm) on the surface of oil–water mixture contained in a Petri dish. All the experiments are carried out at 25 °C on 50 : 50 oil–water mixtures. The adsorption capacity of the material was evaluated in five different oils such as petrol,

Table 1 The formulations of samples with sample codes

Sample code	Sample description
PCL	10% PCL
PCL–5BW	95% PCL + 5% beeswax
PCL–10BW	90% PCL + 10% beeswax
PCL–15BW	85% PCL + 15% beeswax
PCL–20BW	80% PCL + 20% beeswax
PCL–25BW	75% PCL + 25% beeswax

diesel, kerosene, sunflower oil, and gingelly oil. At different time intervals the absorbent weight were monitored to evaluate the absorption kinetics. The absorption capacity (Q) at different time intervals can be calculated by the equation

$$Q_t = \frac{(W_t - W_0)}{W_0} \tag{1}$$

where W_0 is the mass of dry membrane W_t is the total weight of the wet membrane at a particular time t.[39]

2.5. Reusability and recovery

Absorption capacity of PCL/BW electrospun membrane for one min time was monitored for 15 continue cycles in order to evaluate the reusability of the membrane. After each absorption cycle the oil was squeezed with padding paper and washed with ethanol. The recovery percentage (R) of oils were calculated by the following equation,

$$R = \frac{W_r}{(W_e - W_0)} \times 100 \tag{2}$$

where W_r is the weight of collected oil from the membrane, W_0 is the dry weight of membrane, and W_e is weight of membrane after 1 min absorption.

2.6. Gravity driven oil–water separation test

The PCL–25BW membrane was fixed in between two glass tubes with a diameter of 2.5 cm. Mixtures of oil and water (50% v/v) were taken in the upper tube without any applied pressure. The whole apparatus was tilted 45° angle to ensure the oil layer contact with the membrane. During this process, the separation was achieved due to gravity.[44] Three types of oil–water mixtures, such as petrol/water, diesel/water and kerosene/water were analyzed.

Flux was calculated by measuring the amount of oil passed through the membrane for 1 min by using the formula.

$$F = \frac{V}{At} \tag{3}$$

where F is the flux of oil in $Lm^{-2} h^{-1}$, V is the separated volume of oil measured in 1 min (t), A is the contact area of the circular membrane.

The separation efficiency of the membrane was calculated by the formula

$$R = \frac{(V_m + V_s)}{V_o} \times 100 \tag{4}$$

where V_o is the volume of oil before separation, V_s and V_m is the volume of oil after separation and volume of oil adsorbed in membrane respectively. Recyclability test was conducted for 10 cycles for petrol/water mixture. After each cycle, the membrane was washed with ethanol and dried at 30° for 2 h and subjected to oil water flux experiments.

2.7. Durability tests

The PCL/BW membranes are bought under exposure of 15 W mercury lamp with a distance of 20 cm for different time intervals for examining the UV resistance. The UV exposure chamber was kept at the constant condition of 25 °C with a relative humidity of 55%. After exposure, the samples were analyzed for water contact angle. In order to monitor the pH resistance, the membranes are dipped in 15 mL solutions with different pH for 12 h and analysed for surface wettability. Then the membranes were dried at room temperature and the water contact angles were measured.

3. Result and discussion

3.1. Morphology of electrospun PCL/BW nanofibrous membranes

The SEM morphologies of nanofibrous membranes by varying the concentration of BW are shown in Fig. 1. All images revealed
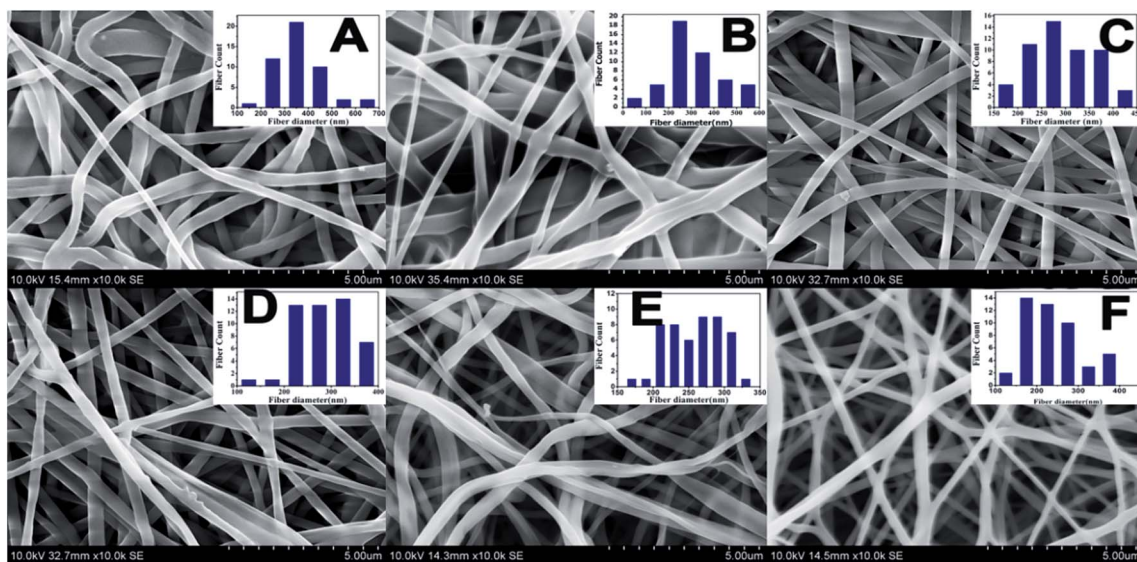

Fig. 1 SEM morphologies of electrospun PCL/BW samples at different beeswax concentrations and fiber diameter distributions. (A) PCL, (B) PCL−5BW, (C) PCL−10BW, (D) PCL−15BW, (E) PCL−20BW, (F) PCL−25BW.

the formation of randomly oriented three-dimensional cylindrical nonwoven fibers with diameters ranging from 385 nm to 247 nm. Pristine PCL have an average fiber diameter of 385 ± 25 nm. A remarkable decrease in average fiber diameter is noticed with increase in beeswax concentration (Fig. 1B–F). Membrane with 5 wt% of BW has a fiber diameter of 331 ± 30 nm and 25 wt% BW has the lowest fiber diameter of 247 ± 34 nm. Fig. 2 histogram, illustrates the variation in average fiber diameter with respect to BW concentration. This dramatic decrease in average fiber diameter is due to the excellent miscibility of two hydrophobic matrices. PCL is a hydrophobic polymer with excellent elastic properties and electrospinnability.[40] BW is a naturally occurring lipid having prominent hydrophobic behaviour. It is a long chain hydrocarbon with more than 50 carbon atoms. The major cause of decrease in average fiber diameter with the addition of BW can be explained by the viscosity variation of the spinning dope. A prominent decrease in viscosity of electrospun solution occurs along with the gradual increase of BW concentration in PCL matrix. This phenomenon occurred due to the lower molecular weight of BW compared to PCL. In less viscous solutions the polymer chains are sufficiently isolated and do not overlap, as a result more prominence towards the formation of electrospun fibers with lesser diameter. The lower fiber diameter rough surface observed in PCL–25BW indicated an enhancement of hydrophobic properties.

The surface roughness of PCL/BW electrospun membrane was further confirmed from AFM analysis. Fig. 3 exhibited the AFM images of PCL and PCL–25BW electrospun membranes. The incorporation of beeswax in PCL will reduce the fiber diameter of the electrospun membrane as a result the surface roughness (R_f) increased. Pure PCL electrospun membrane showed a surface roughness of 2.1 nm. Also PCL–5BW, PCL–10BW, PCL–15BW, and PCL–20BW showed a gradual increase average surface roughness (R_a) of 5.5 nm, 5.9 nm, 9.5 nm, and 15.7 nm respectively (Fig. S4†). PCL–25BW membrane exhibited higher R_a of 19.1 nm. It could be observed that beeswax concentration increases from 0 wt% to 25 wt% induces a significant increase in R_a of PCL–BW nanofiber membranes.
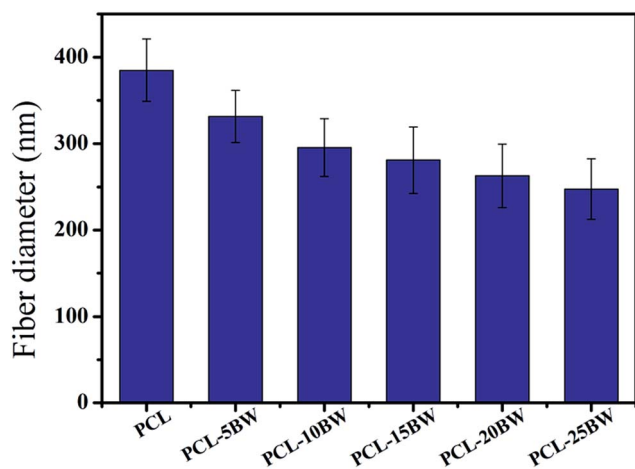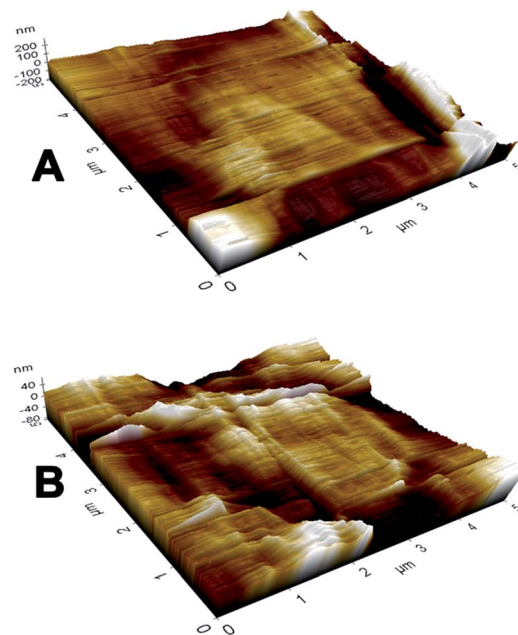

Fig. 3 AFM images of (A) PCL and (B) PCL–25BW electrospun membranes.

3.2. IR analysis

Fig. 4A illustrated the transmission spectra of pristine PCL, beeswax, and PCL–25BW electrospun membranes in the 400–4000 cm^{-1} regions. The characteristic absorption band of PCL appeared at 1725 cm^{-1} corresponding to the carbonyl stretching mode and peaks at 2946 cm^{-1} and 2864 cm^{-1} were due to

Fig. 2 Average fiber diameter of various concentrations of PCL/BW electrospun fibers.
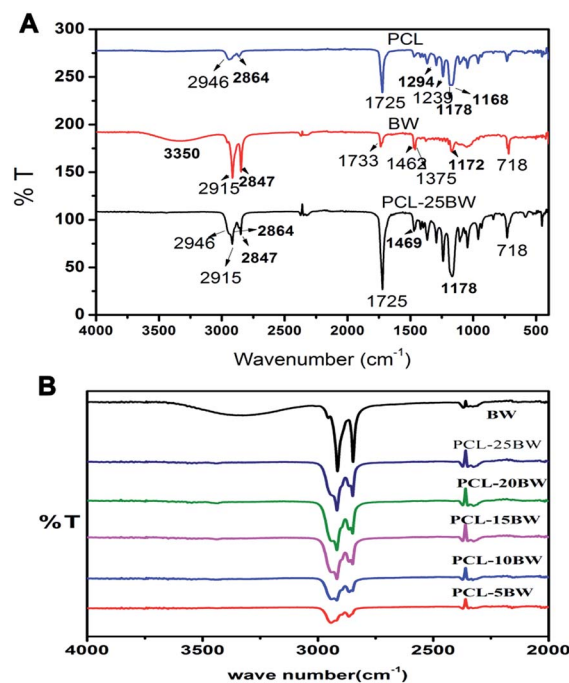

Fig. 4 IR spectra of (A) PCL, beeswax, and PCL–25BW, (B) IR spectra, increment of C–H stretching peak with increase in beeswax concentration and variation in peak area with beeswax concentration.

symmetric and asymmetric stretching of C–H bond. The peak at 1294 cm^{-1} was assigned to the backbone C–C and C–O stretching modes in the crystalline phase of PCL and the peaks at 1178 cm^{-1} and 1168 cm^{-1} is due to symmetric C–O–C stretching and C–O, C–C stretching in amorphous phase respectively. Beeswax exhibited a broad OH stretching peak at 3350 cm^{-1} and asymmetric C–H stretching peak of CH$_3$ was observed at 2915 cm^{-1}. A sharp peak at 1733 cm^{-1} denoted the lipid absorption arises from the C=O group of cholesterol ester. Peaks at 1462 cm^{-1} and 1375 cm^{-1} showed CH$_2$ bending and CH$_3$ asymmetric deformations, and peak at 718 cm^{-1} denoted the CH$_2$ rocking.

IR spectra of PCL–25BW showed all characteristic peaks of PCL and BW. Fig. 4B illustrates the increase in the intensity of C–H stretching peak at 2915 cm^{-1} with increase in beeswax concentration in PCL matrix.

3.3. Superhydrophobic behaviour

The pristine PCL was a hydrophobic polymer with a lower surface energy value of 20 mJ m^{-2}.[41] Therefore PCL electrospun membrane has been exhibited a water contact angle (WCA) of 127 ± 2° and water drops remained on the surface of the samples for a long time. The inclusion of BW in PCL has showed a significant increase in WCA towards superhydrophobicity as illustrated in Fig. 5. Wettability was depends on surface topography, surface free energy and chemical composition of the membrane. As the BW concentration increases in PCL matrix, the water contact angle increases gradually due to the decrease in surface free energy and increase in surface roughness. The surface energy values were theoretically calculated and represented in Section S5.† PCL–20BW and PCL–25BW electrospun membranes exhibited very lower surface free energy values of 1.57 mJ m^{-2} and 1.29 mJ m^{-2}. As a result the PCL–20BW and PCL–25BW nonwoven mat show remarkably higher WCA of 149 ± 2° and 153 ± 2°, compared to PCL–5BW and PCL–10BW with contact angles of 132 ± 1° and 133 ± 1° respectively. PCL–20BW and PCL–25BW exceeded superhydrophobic WCA limit. The surface wettability of PCL–25BW membranes has been showed in the Video S1.† PCL–25BW exhibited a decrease in surface energy because of the immobilization of hydrophobic

long-alkyl chain of BW on the surface of the membrane. Also the lowest fiber diameter of PCL–25BW membrane induces an increased surface roughness of 19.1 nm compared to other PCL–BW membranes.

Sliding contact angle (SA) is another parameter to evaluate superhydrophobic behaviour of the membrane. The sliding contact angle also indicates the water–solid interaction and self cleaning characteristic of the membrane. The SA has been determined for different PCL beeswax membranes with 10 μL of water droplet and the platform was tilted at a high angle until the drop started to roll. The SAs of PCL, PCL–5BW, PCL–10BW, PCL–15BW, PCL–20BW and PCL–25BW were 46 ± 2°, 32 ± 2°, 27 ± 2°, 18 ± 2°, 12 ± 2° and 8 ± 2° respectively, indicating a significant decrease of SAs with addition of beeswax. Due to the increase in surface roughness and lower surface energy, pinning of water droplet reduces and gets lower SAs in range of 8° for PCL–25BW membranes. Thus PCL–25BW membranes exhibited the maximum WCA of 153 ± 2° with a lowest SA of 8 ± 2°.

3.4. Tensile property of PCL/BW fibrous membranes

High strength and breaking elongation, good shape recovery and shape retention are the important parameters considered as essential for an efficient and reusable oil sorbent membrane. Fig. 6A represents the stress vs. percentage of elongation curves for different PCL/BW electrospun nanofibrous membranes. The first stage of stress–elongation curves of all the samples exhibited a non-linear elastic behaviour, and then nearly reached in a stabilized higher stage. The non-linear elastic behaviour is due to the slipping of fibers among the fibrous mat under initial stress load. At the second stage, the stress applied would be almost constant and the elongation of the membrane increased continuously before the rapture. This would be due to the complete orientation of random nanofibers on stress loading direction and in second stage the load was induced on the uniform oriented fibers along the direction of extension. The percentage of elongation was increased with-increase in BW concentration in PCL electrospun membrane. Fig. 6A showed that PCL–5BW membrane executes a break at an elongation of 75% and PCL–20BW at 113%. The increase in percentage elongation with increase in concentration of BW indicates that BW inclusion has imparted a considerable increase in membrane flexibility and viscoelastic properties. This dramatic change in elongation percentage is due to the lubricant action of naturally occurring hydrocarbon lipid in between long polymeric chains. BW acts as a lubricant in between high molecular weight PCL molecules and imparts an increased percentage of elongation. But the excess amount of BW imparts waxy brittle behaviour to PCL matrix. Above an optimum concentration the lipid properties of BW predominate over the flexibility PCL–20BW membranes, as a result for PCL–25BW the elongation percentage decreases drastically to 40%.

The tensile strength of the resultant fibrous mats is summarized in Fig. 6B. Inclusion of 5% BW in PCL membrane causes a drastic reduction in tensile strength from 6.5 ± 0.4 MPa to 3.7 ± 0.02 MPa. But further increase in the
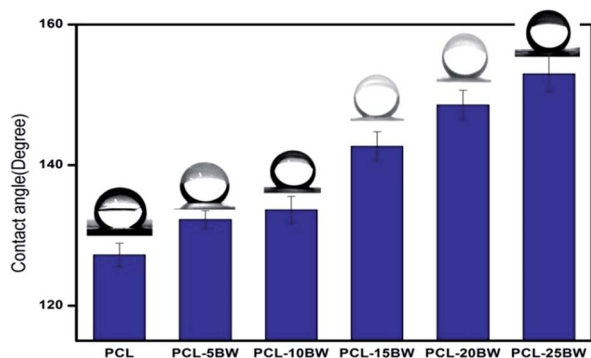

Fig. 5 Variation in water contact angle with the addition of beeswax in PCL electrospun membranes.
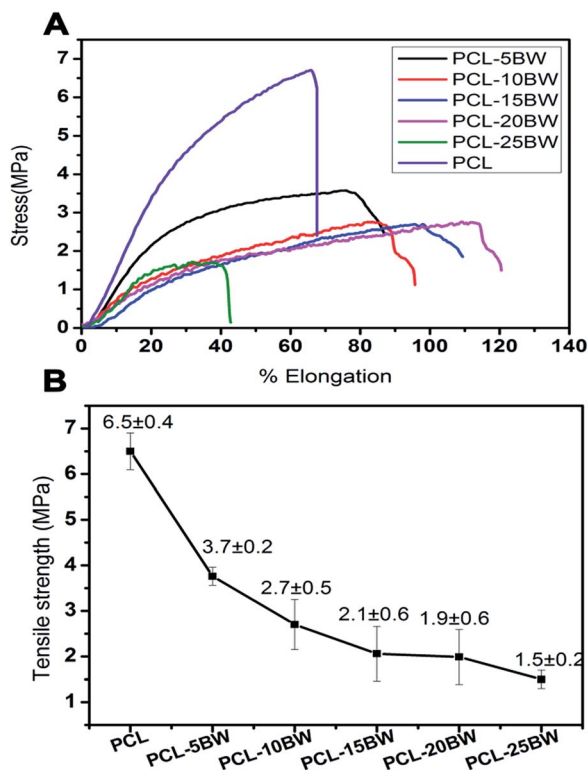
Fig. 6 (A) Stress-percentage vs. elongation curve with different beeswax concentration in PCL/BW electrospun membranes. (B) Variation in tensile strength of PCL/BW electrospun membranes with the addition of various concentration of beeswax.

Fig. 7 (A) TGA curves of PCL−BW electrospun membranes, (B) DTGA curves of PCL−BW electrospun membranes.

concentration of BW from 5% to 25% causes only a slight decrease in tensile strength for electrospun membranes. BW has a low molecular weight lipid behaviour, which occupies in between the high molecular weight long polymer chains and act as a lubricant. The lipid nature of BW induces a decrease in intermolecular interactions between long chains of PCL and resulted in lowering of tensile strength. But compared with many other electrospun superhydrophobic membranes such as polystyrene/silicon oil and polystyrene/polyurethane, PCL–25BW exhibited better tensile strength.[38,42] As a result PCL–25BW can be considered as a promising membrane for effective oil–water sorption.

3.5. TGA analysis

TGA analysis has been carried out for the evaluation of thermal stability of PCL–BW electrospun membranes. Fig. 7A shows TGA curves of BW and different concentrations of electrospun PCL/BW scaffolds. The initial degradation temperature at 2% degradation (T_i), temperature corresponds to 10% weight loss (T_{10}), and temperature for maximum degradation rate (T_{max}) were tested and listed in Table 2. Pristine PCL electrospun fibers exhibit a single degradation stage with T_i at 234 °C, T_{max} of 389 °C leading to the total decomposition. The DTGA curve Fig. 7B illustrates the thermal degradation of beeswax occurs at several stages from 193 °C to 487 °C. Slight increase in degradation temperatures was ascribed by the inclusion of beeswax
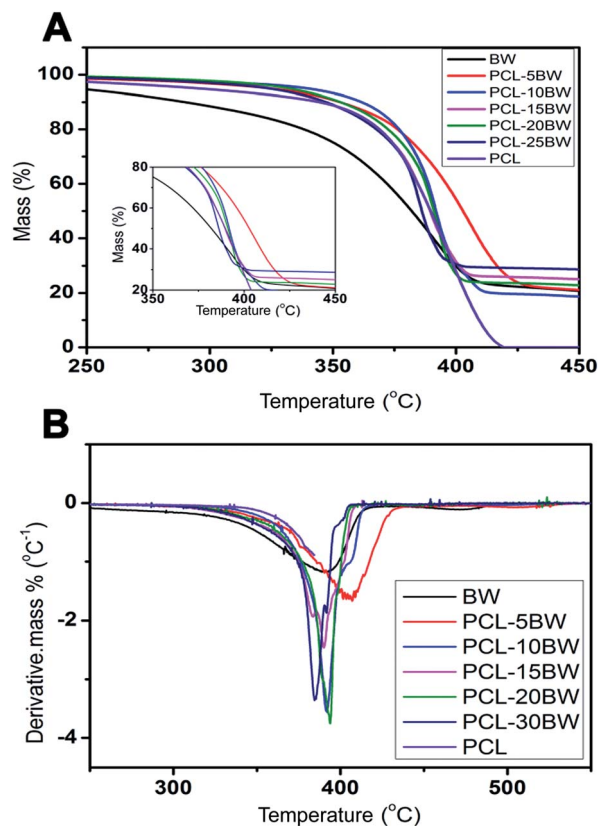
in PCL electrospun matrix (Fig. 7A). All the PCL/BW membranes exhibit a single degradation profile and a large percentage mass loss during TGA analysis.

Presence of the BW causes an important barrier effect, which hinders the diffusion of the degradation products from the bulk of the polymer to the gas phase, as show down their mass loss rate. Also, continues fibrous morphology of the membrane has been found to act as a protective network to reduce the release of decomposition gasses from the polymeric matrix.[43] Fig. 7B provides information about the derivative of TGA thermogram (DTGA) which investigates the effect of BW concentration on degradation temperature. The inclusion of BW in PCL matrix was confirmed by the minor shift observed for PCL/BW in DTGA curve. PCL/BW membrane did not expect any chemical linkage

Table 2 Characteristic degradation temperatures of electrospun PCL−BW membranes

Sample	T_i (°C)	T_{10} (°C)	T_{max} (°C)
BW	193 ± 1	289 ± 1	382 ± 1
PCL	234 ± 1	344 ± 1	389 ± 1
PCL–5BW	271 ± 1	352 ± 1	402 ± 1
PCL–10BW	282 ± 1	361 ± 1	392 ± 1
PCL–15BW	285 ± 1	346 ± 1	389 ± 1
PCL–20BW	295 ± 1	352 ± 1	391 ± 1
PCL–25BW	279 ± 1	347 ± 1	385 ± 1

between PCL and BW, but the slight shift in DTGA might be due to the enhancement of surface interaction and miscibility between PCL and BW.

3.6. Oil sorption capacity

PCL/BW electrospun membranes with different BW concentration were evaluated for oil sorption capacity. PCL–20BW and PCL–25BW membrane exhibited superhydrophobic behaviour with WCA of $149 \pm 2°$ and $153 \pm 2°$ respectively. As expected from WCA analysis, PCL–20BW and PCL–25BW showed excellent oleophilicity and high selective oil sorption capacities from water surface. PCL–25BW membranes exhibited high porosity of 83.8% (Section S3†), also facilitates the capillary action during oil sorption. Fig. 8A–F demonstrates the photograph of selective sorption of oil from the water surface (Video S2†).

1 mL of sunflower oil labelled with red oil colour was placed on a Perti dish filled with water. 3 cm^2 dimension of PCL–25BW rectangular membrane with thickness 0.13 mm was brought in contact with the floating thin oil layer on the water surface, the membrane rapidly sorbs the oil while repelling the water as illustrated in Fig. 8D. Thus the oil layer was completely removed by membrane sorption and the water surface completely cleared (Fig. 8F).

Fig. 8G illustrated the saturated oil sorption capacity of different PCL/BW membranes. PCL, PCL–5BW, PCL–10BW and PCL–15BW electrospun membranes showed minimum saturated oil sorption capacity due to comparatively low porosity and oil molecules occupies only in external pore of membranes without solvation (Fig. S3†). The pristine PCL electrospun membranes showed a minimal oil sorption capacity in the range of $2.26–8.14$ g g^{-1} for different oils. With the inclusion of 25% beeswax in PCL matrix the oil sorption capacity of electrospun membranes gradually increases to $16.95–31.05$ g g^{-1} for different oils. This phenomenon can be explained with reference to increase in hydrophobicity and porosity (83.8%) of PCL–25BW with an average pore diameter of 1703 nm. As a result the interconnected pore density of the membrane increases. Compared to pristine PCL electrospun membrane PCL–25BW

membranes showed an increase in saturated oil sorption capacity, 533% for petrol, 436% for diesel, 815% for kerosene, 309% for gingelly oil and 281% for sunflower oil.

The oil sorption kinetics of electrospun membranes have been studied by various oil–water mixtures such as petrol–water, diesel–water, kerosene–water, gingerly oil–water and sunflower oil–water are showed in Fig. 9. Oil sorption kinetics is an essential parameter considering a sorbent material. An effective sorbent should attain sorption equilibrium by penetration of solvents into the interconnected pores of the membrane with a short time.[43] The pore density of PCL, PCL–5BW, PCL–10BW, PCL–15BW, PCL–20BW and PCL–25BW were 73.8%, 78.5%, 80.5% 81.4%, 82.1% and 83.8% respectively (Section S3†).

For oils with low viscosity such as petrol, diesel (2.6 cP) and kerosene (1.64 cP) the membrane attained sorption equilibrium in 3 min. But in the case of highly viscous oils such as gingelly oil (65 cP) and sunflower oil (68 cP) the sorption equilibrium extended to 10 min. The oil sorption capacity of the electrospun nanofibrous membranes is due to the combination of different phenomena such as absorption, adsorption and capillary action. The first step of oil sorption in electrospun membrane was physical adsorption, then trapping of solvent at the inner pores of the membrane by capillary action. As a result the low viscosity oils quickly moved into the inner voids and attained fast sorption equilibrium compared to highly viscous oils. The oil sorption kinetics graph demonstrated a variation in oil sorption capacity with respect to the viscosity of different oils. The oil with lower viscosity easily desorbed from the inner pores during the draining period, on other hands highly viscous oils trapped in inner voids would not desorbs easily. PCL–20BW and PCL–25BW exhibited superhydrophobicity and high porosity of 82.1% and 86.8%, as a result they showed much higher oil sorption capacities compared with some surface-modified nanomaterials, such as foams, nanocomposites, nanocellulose aerogels, nanoparticles, and nanowires synthesized through a series of complex processing procedures.[44–47] After 30 min of oil adsorption the membranes exhibited improved tensile strength of 4.35 MPa. This would be due to the fibre swelling
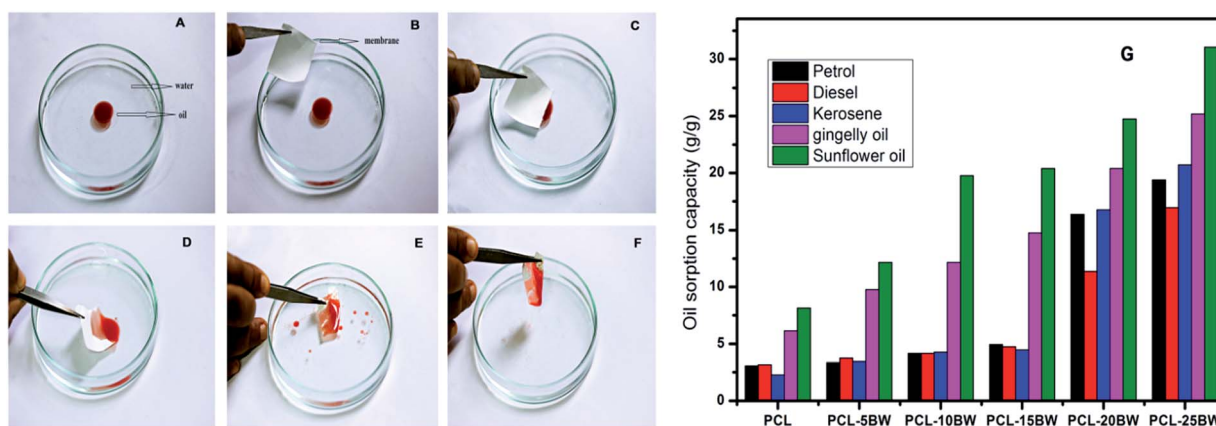

Fig. 8 (A–F) Photographs of selective sorption of oil from water surface with PCL–25BW membranes. (G) Saturated oil sorption capacity of various concentrations of PCL–BW electrospun membranes in different oils.
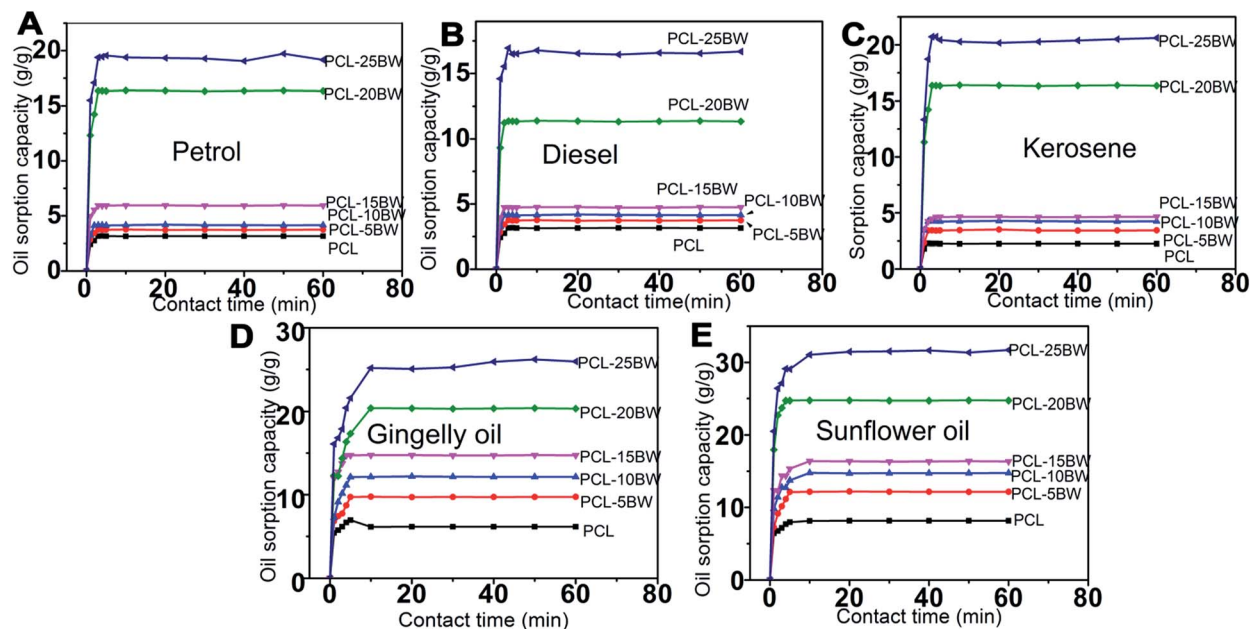
Fig. 9 Absorption kinetic of PCL−BW electrospun membranes in various oil−water mixtures: (A) petrol−water mixture; (B) diesel−water mixture; (C) kerosene−water mixture; (D) gingelly oil−water mixture; (E) sunflower oil−mixture.

and adhesion occurred during sorption. These results are promising for fabrication of oil–water sorption electrospun membranes.

3.7. Recyclability

The reusability of PCL–25BW nanofibrous membranes was examined for fifteen sorption cycles with different oil–water mixture and the trend was illustrated in Fig. 10. After each cycle, the sorbed oil on the electrospun membrane was removed by rinsing with ethanol followed by drying. The average recoveries for petrol, diesel, kerosene, gingelly oil and sunflower oil are 93.0%, 87.8%, 78.1%, 84.0% and 71.8%, respectively (Fig. 10). After 15 sorption cycles the PCL–25BW membrane exhibited a decrease in sorption efficiency 24.8% for petrol, 45.1% for diesel, 65.70% for kerosene, 49.1% for gingelly oil and 49.6% for sunflower oil. The PCL–25BW membrane exhibited a water contact angle of 149 ± 2° and tensile strength of 2.85 MPa even after 15 cycles of oil sorption. Fig. 10F exhibited the SEM morphology of PCL–25BW electrospun membranes after 15 absorption cycles in kerosene. This SEM image gives a confirmation about the retention of fibrous morphology of PCL–25BW membrane with fiber diameter of 734 ± 170 nm even after 15 absorption cycles. The slight increase in tensile strength of PCL–25BW after 15 sorption cycle is due to the drastic increase in fiber diameter and adhesion between the fibers. Reusability and recovery percentage of the PCL–25BW membrane confirms high chemical and mechanical stability in various oils. Theoretically, 1 kg of membrane can recover almost 174 kg petrol, 186 kg of diesel, 186 kg kerosene, 282 kg of gingelly oil, 264 kg sunflower oil in 15 cycles. The result indicates that membrane modified by BW is a promising material for reusable oil/water separation.

3.8. Gravity driven oil water separation

PCL–25BW membranes have a great potential in gravity driven oil–water separation due to its superhydrophobic behaviour. The membrane supported with no other membranes has been examined for oil flux analysis. It exhibited gravity driven oil flux of 1599 Lm^{-2} h^{-1}, 1066 Lm^{-2} h^{-1}, 1492 Lm^{-2} h^{-1} respectively against petrol, diesel and kerosene. For high viscosity-oils such as gingelly oil and sunflower oil the membrane showed a low flux of 27 Lm^{-2} h^{-1}. Light oil–water mixtures were also examined for gravity driven flux analysis and showed in Fig. 11A–C (Video S3†). Mixture of petrol (yellow) and water were poured onto the PCL–25BW membranes clamped in between two glass tubes. The setup was placed obliquely such that petrol could come into contact with the membrane. Due to the superhydrophobic and superoleophilic character of PCL–25BW membranes, petrol quickly permeated through the membrane and dropped into the beaker meanwhile, water stay above the membrane. During this process-the light oil layer was only in partial contact with the membrane, also the pressure due to gravity was partially applicable, as a result the oil flux of light oil–water mixture decreases compared to actual oil flux. Petrol–water mixture showed a flux of 359 Lm^{-2} h^{-1}. Diesel–water and kerosene–water mixture successfully analysed by the same process with flux values of 331 Lm^{-2} h^{-1} and 248 Lm^{-2} h^{-1}. Fig. 11D showed the flux of petrol–water mixture during 10 cycles. From 5th cycle onwards the flux of PCL–25BW membranes slightly decreases due to the partial destruction of fibrous morphology.

The SEM images of PCL–25BW electrospun membrane after 10 separation cycles were showed in Fig. 11G. It confirms that after 10 separation cycles, swelling of nanofibers and destruction of fibrous morphology occurs, which decreases the pore
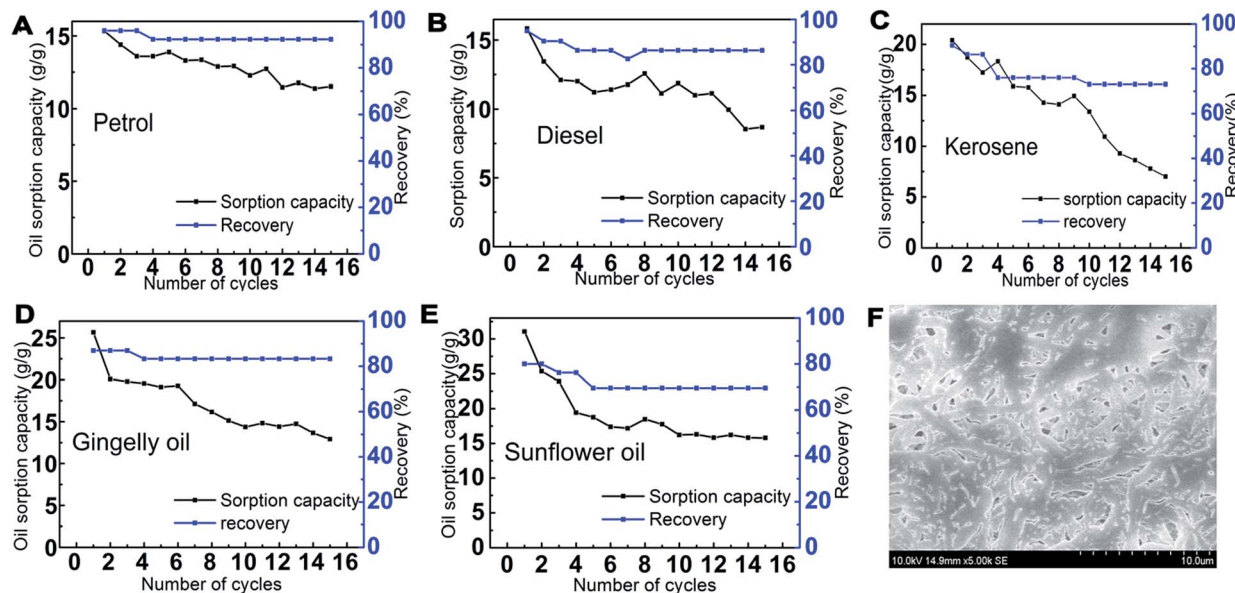
Fig. 10 Reusability and recovery percentage of the PCL−25BW membranes in (A) petrol, (B) diesel, (C) kerosene, (D) gingelly oil, (E) sunflower oil, (F) SEM image of PCL−BW membranes after 15 absorption cycles in kerosene.
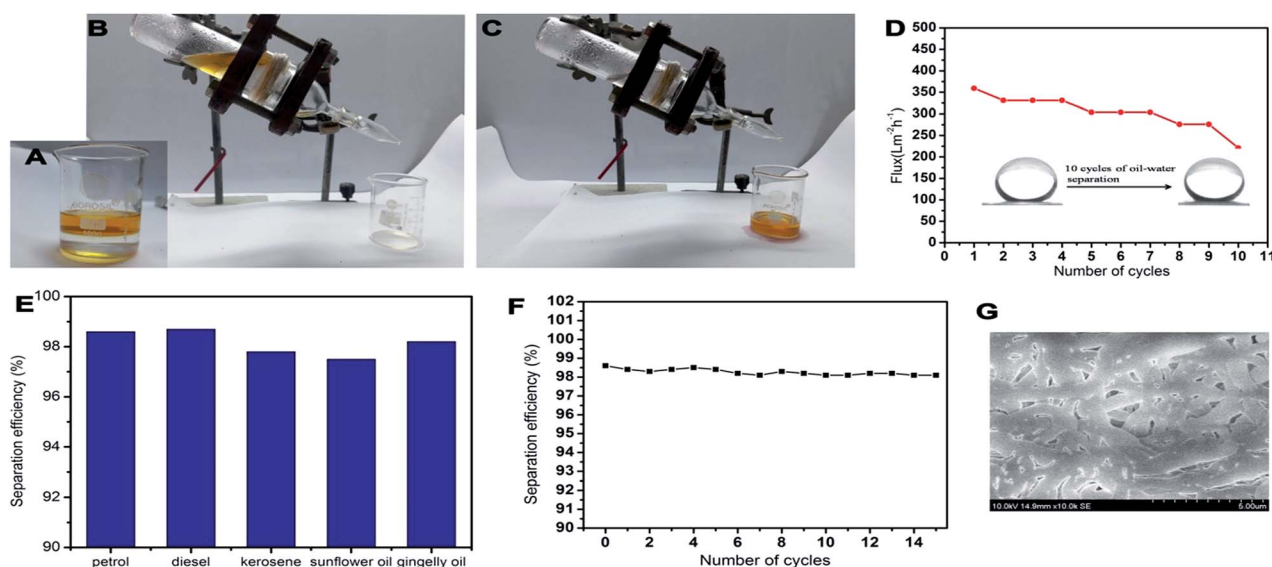

Fig. 11 (A−C) Gravity-driven petrol/water separation setup. (D) Changes in petrol−water flux with 10 cycles of separation and WCA images of the PCL−25BW surface before petrol−water separation and after 10 separation cycles (E) variations of oil separation efficiency in different types of oil/water mixtures. (F) separation efficiency of kerosene at 15 cycles of separation (G) SEM image of PCL−25BW membranes after 10 cycles of separation.

density of the membrane. But the WCA of the PCL–25BW surface after ten times of separation is $152 \pm 2°$. This reveals the maintenance of superhydrophobic nature of the membrane even after 10 cycles of separation. Fig. 11E illustrated the separation efficiencies of PCL–25BW membranes during gravity driven oil–water separation. The separation efficiency of PCL–25BW membrane was calculated for different oils and showed average of 98.1% for all the light oil–water mixtures, which is highly promising for oil polluted water treatment. The oil/water separation efficiency *versus* the number of cycles was also

investigated by taking the kerosene–water mixture (Fig. 11F). The PCL–25BW membrane exhibited separation efficiency even after 15 cycles. These results confirmed that the PCL–25BW membrane has an excellent potential in removing oil pollutants from water.

3.9. Durability

The durability and stability under harsh condition are important parameters that support towards the practical applications of oil sorbent material in oil spill accidents. The PCL–25BW
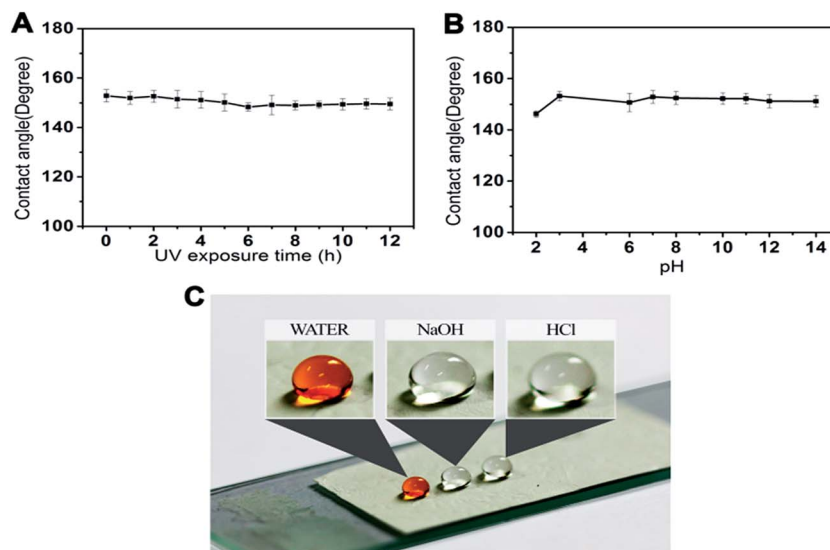
Fig. 12 (A) Contact angles of PCL–25BW membrane under different time of UV exposure and (B) different pH (C) photographs of water drop, 1 M-NaOH drop and 1 M-HCl drop.

superhydrophobic electrospun membranes undergone durability check for different UV exposure times and pH ranges. Fig. 12A shows the variation in water contact angle under different UV exposure times. The membrane has been exhibited high UV stability and remains superhydrophobic even after 12 h of exposure time. The contact angle measurements under a pH range of 2–14 were illustrated in Fig. 12B. PCL–25BW membranes showed superhydrophobic behaviour from a pH range of 3–14. The membranes were dipped in 1 M-NaOH, 1 M-HCl, and 1 M-NaCl in order to check the stability under acidic basic and neutral condition and found that the membrane remains superhydrophobic with-contact angles of $150 \pm 1°$, $151 \pm 1°$, and $151 \pm 1°$ respectively even after 24 h immersion time. Fig. 12C is the photographs showing contact angle of the membrane with water droplet, 1 M NaOH and 1 M HCL droplet. From the above result, it can be concluded that the PCL–25BW membrane shows high resistance from water corrosion even in high acidic and basic conditions indicating that PCL–25BW membrane is an excellent candidate for oil water sorption in harsh conditions.

4. Conclusion

In summary, we have demonstrated the fabrication of a new type of environment-friendly, superhydrophobic electrospun membrane from PCL and beeswax. The wettability of PCL membrane can be easily manipulated from hydrophobic to superhydrophobic by the incorporation of beeswax. The resulting membrane with 25 wt% of BW concentration produces nanofibers with rough surface structure and have a water contact angle of $153 \pm 2°$. The resulting membrane showed a higher thermal stability (393–378 °C) and good mechanical strength of 1.5 MPa. PCL–25BW showed higher sorption capacity for gingelly (25.17 g g^{-1}) and sunflower oil (31.05 g g^{-1}) than petrol (149.38 g g^{-1}), kerosene (20.72 g g^{-1})

and diesel (16.95 g g^{-1}) compared to pristine PCL electrospun membrane. Even after fifteen sorption cycles, the electrospun membrane showed a higher sorption capacity. Gravity driven oil–water separation of PCL–25BW exhibited high flux and high separation efficiency of 98.1%. Moreover, the PCL–25BW membranes are highly stable at harsh environmental conditions such as UV exposure and pH. This study explores a new area of superhydrophobic hybrid membrane with beeswax as a functional material for selective oil/water separation.

References

1 S. Yu, Z. Guo and W. Liu, *Chem. Commun.*, 2015, **51**, 1775–1794.
2 C. H. Xue, X. J. Guo, J. Z. Ma and S. T. Jia, *ACS Appl. Mater. Interfaces*, 2015, **7**, 8251–8259.
3 C. Liu, F. Su and J. Liang, *RSC Adv.*, 2014, **4**, 55556–55564.
4 T. Ishizaki, Y. Masuda and M. Sakamoto, *Langmuir*, 2011, **27**, 4780–4788.
5 T. C. Huang, P. Li, H. Yao, H. J. Sue, M. Kotaki and M. H. Tsai, *RSC Adv.*, 2016, **6**, 12431–12434.
6 W. Zhang, X. Lu, Z. Xin and C. Zhou, *Nanoscale*, 2015, **7**, 19476–19483.
7 J. Li, D. Li, Y. Yang, J. Li, F. Zha and Z. Lee, *Green Chem.*, 2016, **18**, 541–549.
8 S. Nagappan, J. J. Park, S. S. Park, W. K. Lee and C. S. Ha, *J. Mater. Chem. A*, 2013, **1**, 6761–6769.
9 S. Kheradmandnia, E. V. Farahani, M. Nosrati and F. Atyabi, *Nanomedicine*, 2010, **6**, 753–759.
10 A. A. Attama and C. C. M. Goymann, *Colloids Surf., A*, 2008, **315**, 189–195.
11 E. R. H. S. S. Ediriweera and N. Y. S. Premarathna, *AYU*, 2012, **33**(2), 178–182.
12 M. J. Fabra, P. Talens and A. Chiralt, *Food Hydrocolloids*, 2009, **23**, 676–683.

13 H. M. Nguyen, I. C. Hwang, J. W. Park and H. J. Park, *Pest Manage. Sci.*, 2012, **68**, 1062–1068.

14 L. Ren, Y. Cai, L. Ren and H. Yang, *Materials*, 2016, **9**, 1–11.

15 T. Espolov, J. Ukibayev, Z. Wewei, L. Peng, Q. Liying and X. Huining, *Chem. Eng. J.*, 2014, **250**, 431–436.

16 T. Espolov, J. Ukibayev, D. Myrzakozha, P. Perez-Lopez and Y. Ermolaev, *Nat. Sci.*, 2014, **6**, 871–877.

17 C. Dai, N. Liu, Y. Cao, Y. Chen, F. Lua and L. Feng, *Soft Matter*, 2014, **10**, 8116–8121.

18 L. Yu, G. Hao, S. Zhou and W. Jiang, *RSC Adv.*, 2016, **6**, 24773–24779.

19 Z. Xua, K. Miyazaki and T. Hori, *Appl. Surf. Sci.*, 2016, **370**, 243–251.

20 L. Peng, W. Lei, P. Yu and Y. Luo, *RSC Adv.*, 2016, **6**, 10365–10371.

21 Q. An, Y. Zhang, K. Lv, X. Luan, Q. Zhang and F. Shi, *Nanoscale*, 2015, **7**, 4553–4558.

22 E. Zhang, Z. Cheng, T. Lv, Y. Qiana and Y. Liu, *J. Mater. Chem. A*, 2015, **3**, 13411–13417.

23 L. Liu, C. Chen, S. Yang, H. Xie, M. Gong and X. Xu, *Phys. Chem. Chem. Phys.*, 2016, **18**, 1317–1325.

24 F. Wang, S. Lei, Y. Xu and J. Ou, *ChemPhysChem*, 2015, **16**, 2237–2243.

25 Y. Hou, Z. Wang, J. Guo, H. Shen, H. Zhang, N. Zhao, Y. Zhao, L. Chen, S. Liang, Y. Jin and J. Xu, *J. Mater. Chem. A*, 2015, **3**, 23252–23260.

26 T. C. Huang, P. Li, H. Yao, H. J. Sue, M. Kotaki and M. H. Tsai, *RSC Adv.*, 2016, **6**, 12431–12434.

27 Y. Hou, Z. Wang, J. Guo, H. Shen, H. Zhang, N. Zhao, Y. Zhao, L. Chen, S. Liang, Y. Jinc and J. Xu, *J. Mater. Chem. A*, 2015, **3**, 23252–23260.

28 C. Su, Y. Li, Y. Dai, F. Gao, K. Tang and H. Cao, *Mater. Lett.*, 2016, **170**, 67–71.

29 Z. Zhou and X. F. Wu, *Mater. Lett.*, 2015, **160**, 423–427.

30 M. Huang, Y. Si, X. Tang, Z. Zhu, B. Ding, L. Liu, G. Zheng, W. Luo and J. Yu, *J. Mater. Chem. A*, 2013, **1**, 14071–14074.

31 J. J. Li, L. T. Zhu and Z. H. Luo, *Chem. Eng. J.*, 2016, **287**, 474–481.

32 Y. Guo, D. Tang, E. Zhao, Z. Yu, H. Lv and X. Li, *RSC Adv.*, 2015, **5**, 82789–82799.

33 Y. Qiao, L. Zhao, P. Li, H. Sun and S. Li, *J. Reinf. Plast. Compos.*, 2014, **33**(20), 1849–1858.

34 J. Wang, A. Raza, Y. Si, L. Cui, J. Ge, B. Ding and J. Yu, *Nanoscale*, 2012, **4**, 7549–7556.

35 Y. Shang, Y. Si, A. Raza, L. Yang, X. Mao, B. Ding and J. Yu, *Nanoscale*, 2012, **4**, 7847–7854.

36 S. Ouyang, T. Wang, X. Jia, Y. Chen, J. Yao and S. Wang, *Mater. Des.*, 2016, **96**, 357–363.

37 J. Li, L. Yan, Y. Zhao, F. Zha, Q. Wang and Z. Lei, *Phys. Chem. Chem. Phys.*, 2015, **17**, 6451–6457.

38 J. Lin, F. Tian, Y. Shang, F. Wang, B. Ding, J. Yu and Z. Guo, *Nanoscale*, 2013, **5**, 2745–2755.

39 K. Weihua, H. Yuuki, H. Lei and I. Yoshio, *J. Appl. Polym. Sci.*, 2008, **107**, 1395–1400.

40 F. Croisier, A.-S. Duwez, C. Jérôme, A. F. Léonard, K. O. van der Werf, P. J. Dijkstra and M. L. Bennink, *Acta Biomater.*, 2012, **8**, 218–224.

41 E. N. Bolbasov, M. Rybachuk, A. S. Golovkin, L. V. Antonova, E. V. Shesterikov, A. I. Malchikhina, V. A. Novikov, Y. G. Anissimov and S. I. Tverdokhlebov, *Mater. Lett.*, 2014, **132**, 281–284.

42 S. Yan, W. Lige, W. Xiuling, B. Kun, Y. Qingbiao and L. Yaoxian, *J. Appl. Polym. Sci.*, 2014, **131**, 40718.

43 M. D. Ana and G. David, *ACS Appl. Mater. Interfaces*, 2013, **27**, 12107–12119.

44 P. Yanxiong, S. Kai, P. Chao, W. Weicai, L. Zhi and J. Xiangling, *ACS Appl. Mater. Interfaces*, 2014, **6**, 8651–8659.

45 Y. Liuhua, H. Gazi, Z. Shuai and J. Wei, *RSC Adv.*, 2016, **6**, 24773–24779.

46 N. Saravanan, J. P. Jin, S. P. Sung, K. L. Won and S. H. Chang, *J. Mater. Chem.*, 2013, **1**, 6761–6769.

47 X. Zhongxin, S. Zhongxue, C. Yingze, C. Yuning, T. Lei, L. Kan, F. Lin, F. Qiang and W. Yen, *RSC Adv.*, 2013, **3**, 23432–23437.